3.5 Fossil-Fueled Power Plant

Modeling of power plants is of interest for three reasons: (1) it demonstrates the issues involved in chemical, thermodynamic and fluid modeling of industrial processes; (2) it demonstrates the methods required to develop good reduced-order models of a complex system (a requirement for real-time model predictive control); and (3) unlike orbital dynamics, the model must be partly stochastic because deterministic models do not completely capture many small-scale nonlinear and lag effects.

The objective of the research described here was to develop and demonstrate the application of *nonlinear model predictive control* (NMPC) algorithms based on a simplified quasi-generic first-principles (mass and energy balance) model of the plant boiler and turbines (see Gibbs et al. 1991, Gibbs and Weber 1992a, 1992b, Gibbs 1995). Compared with other linearized MPC approaches, NMPC has the potential to provide better control over a wider range of operating conditions, adapt to changing plant conditions, allow greater flexibility in optimization strategies and provide diagnostic information on plant performance. The specific goal of the NMPC effort was to replace existing high-level energy and power controls with optimal controls computed using (1) a Kalman filter that tracked plant performance, and (2) a simplified plant model that allowed prediction of plant responses to control changes. The plants used in the study were two gas-fired 330 MW subcritical drum units located in El Segundo, California. The plants operate at a main steam pressure of 2410 lbf/in^2 (psig)—well below the water critical pressure of 3204 lbf/in^2 absolute (the pressure at which water no longer changes from liquid to steam at a constant temperature). Note that English units are used in this example because all plant input, output, and physical data are in these units.

3.5.1 Plant Description

Figure 3.5-1 shows the general layout of the plant and Figure 3.5-2 shows the simplified water/steam path. Water from the condenser is preheated and pumped at 2700 psig through three additional feedwater heaters (using steam extracted from the turbines) and an economizer (heat exchanger) located in the back pass of the furnace. The economizer output is fed to the 60-inch diameter drum, where it mixes with the drum water. The drum water passes through the downcomers to three circulation pumps that supply a smaller drum that supplies the main furnace waterwall tubes and the extended sidewall tubes. The water/steam mixture (quality ~15% at full load) exiting the waterwall passes through risers back to the drum. Two rows of turbo-separators separate the water from the steam, ensuring that the steam above the waterline is saturated (quality = 100%). This furnace is unusual in that the burners are at the top and the gas flows down to the bottom where it passes to the superheaters.
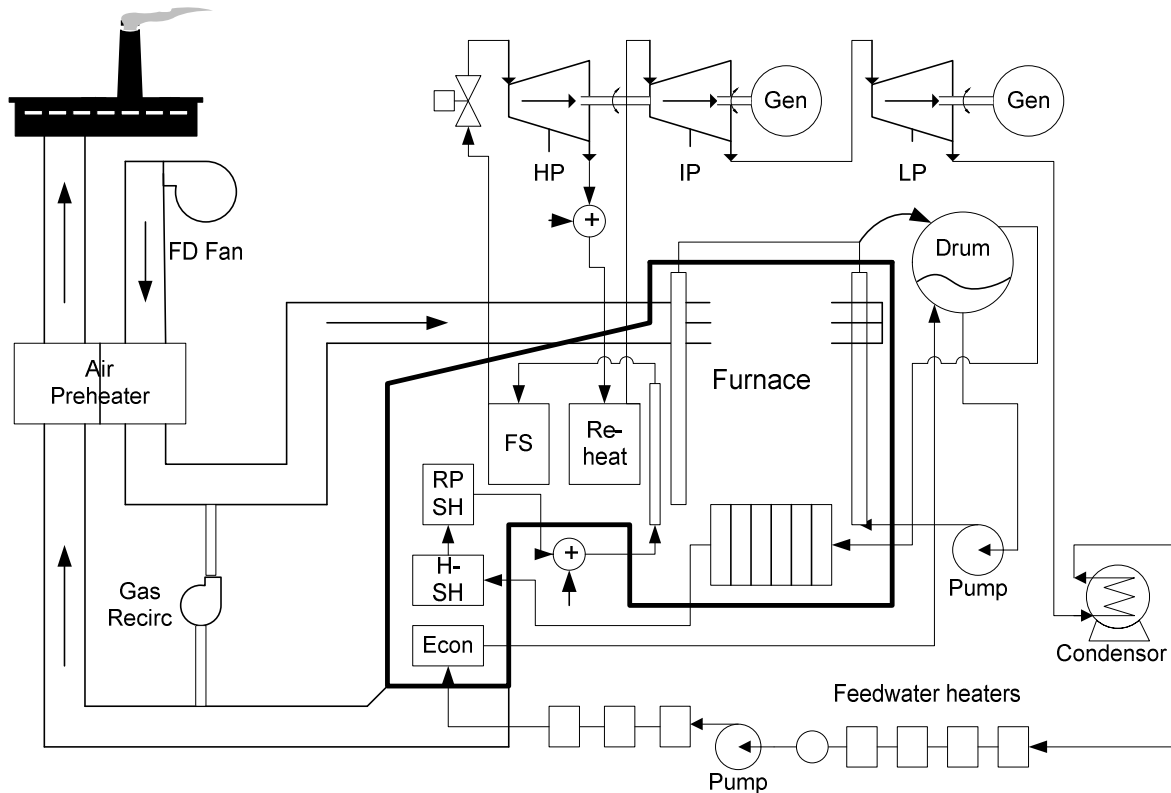
Figure 3.5-1: 330 MW gas-fired subcritical drum power plant.

The steam exiting the drum passes through front wall radiant superheaters located in the bottom of the furnace, and from there to the horizontal and rear pendant superheaters in the backpass. At this point the steam is mixed with water (taken from the feedwater pump outlet) in four attemperator sprays that are regulated to adjust the steam temperature. Steam then passes through the platen superheater and front platen superheater before arriving at the high-pressure (HP) turbine with a temperature of 1050^oF. The heat transfer is primarily convective for all superheaters except the radiant and platen. Four throttling valves regulate the steam flow through the governor stage. Then the steam passes through six more HP stages. All stages in the HP, intermediate-pressure (IP), and low-pressure (LP) turbines are described as "impulse," rather than "reactive." Steam for the first two feedwater heaters is extracted from the middle HP stage and at the HP outlet. These and several other flow paths are not shown in the simplified diagram of Figure 3.5-2.

The steam at the cold reheat header is fed back to the furnace where a reheat spray regulates the steam temperature before passing through the reheater. The source of the spray water is a tap on the boiler feed pump. The reheater is located between the platen and front pendant superheaters. The steam in the hot reheat header passes through four stages of the IP turbine, where steam is extracted after the second and fourth stage. Passing through a crossover tube, the steam follows through eight stages of the LP turbine before returning to the condenser.

Note that the HP and IP turbine are on a common shaft that drives one generator. The boiler feed pump is also on this same shaft separated by a hydraulic coupling to vary speed and regulate water flow. The LP turbine drives a separate generator.

The simplified air/gas path for one-half of the furnace is shown in Figure 3.5-3. Two *forced draft* (FD) fans supply ambient air through two separate drum air preheaters. The FD fan speeds are controlled by hydraulic couplings, and outlet dampers maintain sufficient exit pressure for seal air. Heated air exiting the preheaters passes through air foils (which measure airflow) and then the air is separated into primary and auxiliary air ducts. Air in the primary ducts is fed directly to the three burner elevations where it is mixed with the fuel (gas and/or oil) and ignited in tangentially firing burners. Primary air dampers prevent excessive airflow for the given gas header pressure. Air in the auxiliary air ducts is mixed with recirculated gas supplied by constant speed centrifugal gas recirculation fans with inlet vane control and outlet dampers. The recirculated gas is supplied from a tap located after the economizer. The air/gas mixture in the auxiliary air ducts is fed to overfire air ports located above and below the burners. Auxiliary air dampers are used to regulate the windbox-to-furnace differential pressure (the set point varies with power output). There are a total of 24 burners in the furnace: three elevations, four corners, and two halves.

The air/gas path is physically partitioned in half from the FD fans to the rear wall of the furnace. It has been observed, however, that the flow from the two halves does not mix significantly even at the economizer. For most efficient operation, the furnaces are operated balanced, and crossover ducts in the hot air, gas recirculation, and exit gas paths help in balancing. After leaving the economizer, the hot gas passes through the air preheater (where it heats the incoming air) and exits up the stack.
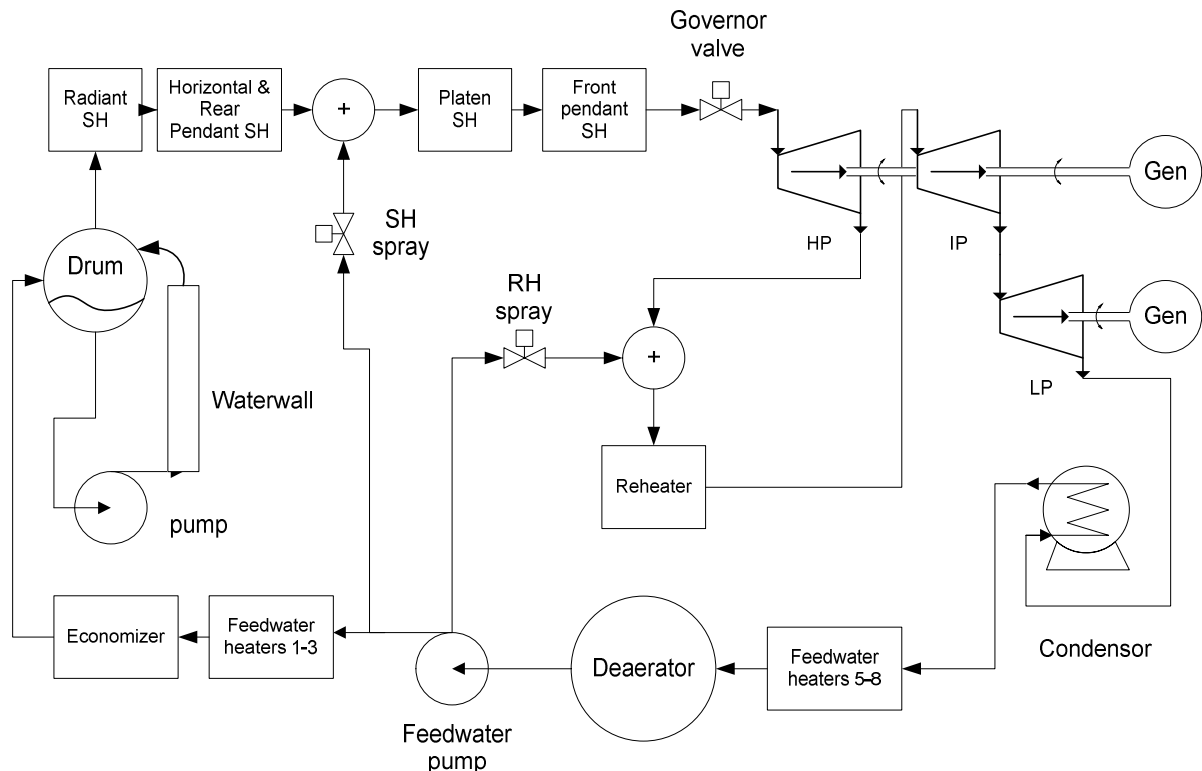
Figure 3.5-2: Simplified water/steam flow path.
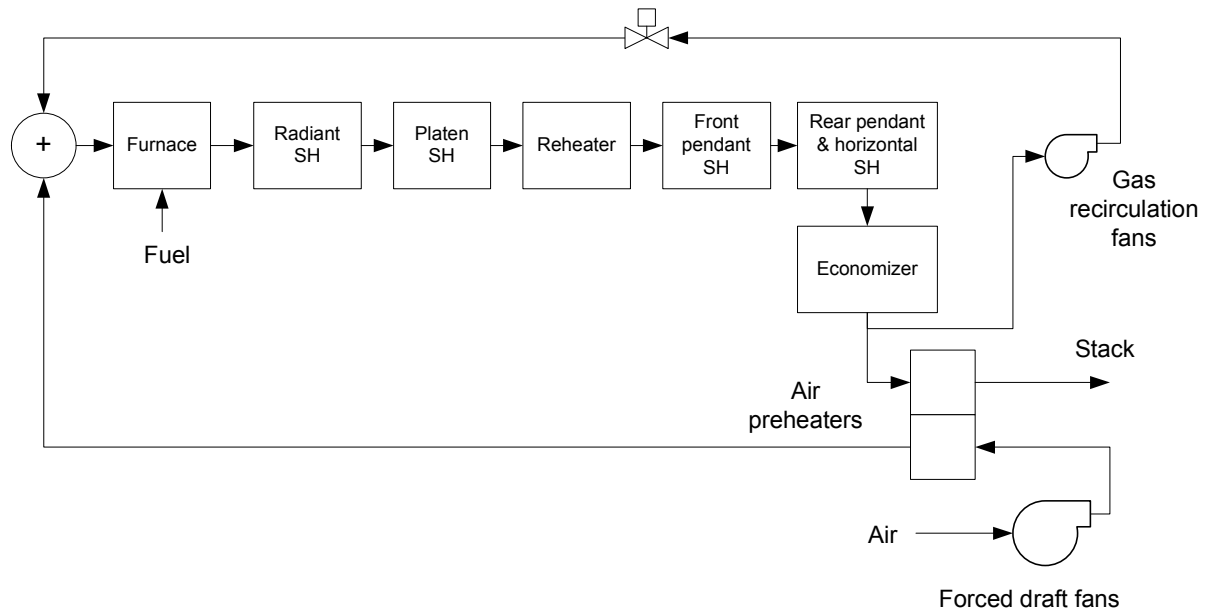
Figure 3.5-3: Simplified air/gas path.

The plant is difficult to model because the water/steam and gas paths tend to occur in opposite directions and the performance of any individual heat exchanger affects the entire plant. Furthermore actuators (fans, pumps, dampers, fluid couplings, etc.) have very nonlinear characteristics. On the positive side, most actuators have output sensors and local control loops so that the "controlled" behavior is nearly linear. Furthermore, the plant is very well instrumented with hundreds of sensors: 287 were used in the study.

3.5.2 Plant Modeling Approach

A detailed model of the plant was independently developed by the plant operators using a commercial process simulation product suitable for power plants, or pulp and paper processing. The simulation model had 234 states that included not only air/gas/water/steam energy and flow-related parameters and metal temperatures, but also actuator and local control loops. It also optionally modeled high-level control loops including drum water level, main-steam pressure, main-steam and hot reheat temperatures, excess oxygen in the exit gas, burner tilt, and generator power output. (These are the control loops to be replaced by MPC.) This simulation was primarily used by the plant operators for engineering analysis and training purposes. It was helpful for testing concepts and performance of the MPC algorithms, but was not, by itself, useful as a model for MPC. For example, the steady-state simulation performance did not match actual plant data, so it was necessary to adjust various coefficients (air/gas and water/steam flow, furnace and air preheater heat transfer, turbine flow and efficiency) by trial-and-error until performance was satisfactory. However, the more serious problem was the model order. Since MPC must integrate the system model for some period in the future at each control step in order to compute the optimal controls, the model order must be low. The *reduced-order model* (ROM) must capture the dominant static and dynamic behavior of the plant within the frequency band that can be controlled, but it should not model high-frequency behavior that is outside the control bandwidth. Process noise in the Kalman filter partially compensates for these ignored high-frequency effects. The ROM must not have any significant biases between modeled and actual

4

behavior. This implies that the model should include "tuning" parameters that can be adjusted on-line by the Kalman filter so that model behavior is unbiased.

For purposes of estimation and control, it is neither necessary nor desirable to use a detailed plant model. It was suspected (and later verified) that a model capturing the dominant behavior of the plant for 60 s predictions was adequate for MPC, and that short term behavior of a few seconds could be ignored. The general approach develops models using first-principles concepts, but applies simplifying assumptions to reduce complexity of the model, as suggested by Balchen and Mummé (1988) and Balchen et al. (1988). For example, the air/gas flow response to control changes is quite rapid (fractional seconds) and was modeled statically rather than dynamically. Also, heat exchangers were modeled by their "lumped" input/output characteristics. The modeling approach is based on fundamental first-principles concepts that may be found in many reference books. For example, see Van Wylen and Sonntag (1986) for thermodynamics; White (1986) for heat and mass transfer; Salisbury (1974), Spencer et al. (1974), and Kearton (1951) for steam turbine modeling; Stultz and Kitto (2007) and Singer (1991) for fossil-fueled power plant design; and Avallone and Baumeister (1996) for general mechanical engineering principles. References on modeling boilers and power plants include Tyssø (1981), Tyssø and Brembo (1976, 1978), Ipakchi et al. (1989), Moore and Schweppe (1973), Weber (1991), Greco and Marchis (1982), Eklund and Gustavsson (1973), Nakamura et al. (1979), Nakamura and Akaike (1981), Kwan and Anderson (1970) and Masada and Wormley (1982). Other references on model predictive control include Balchen et al. (1988) and Morari et al. (1988).

The final model had 13 "core" states (Table 3.5-1) with 104 fixed parameters. The notation and units used in the equations to follow are described below:

1. water flow = w (lbm/s)
2. steam flow = f (lbm/s)
3. air/gas flow = g (lbm/s)
4. enthalpy = h (BTU/lbm)
5. energy transfer = $\dot{Q}$ (BTU/s)
6. pressure = P (psi)
7. electric power = P_{MW} (megawatts)
8. density = ρ (lbm/cu-ft)
9. temperature = T (Rankine)
10. specific heat = C_p (BTU/lbm-R)
11. constants are denoted by K with a subscript
12. input and output quantities are denoted by subscripts i and o, respectively.

Although use of metric units is generally encouraged, in this case all plant measurements and engineering data were provided in English units, so the convention was retained.

Table 3.5-1: 13-state simplified model of subcritical drum plant

	State	Symbol
1	Economizer exit water enthalpy	h_{ecwo}
2	Waterwall riser water/steam enthalpy	h_{rifo}
3	Drum water enthalpy	h_{drmw}
4	Drum water level	w_{lev}
5	Drum pressure	P_{drm}
6	Radiant superheater exit steam enthalpy	h_{rsfo}
7	Rear pendant superheater exit steam enthalpy	h_{hsfo}
8	Platen superheater exit steam enthalpy	h_{plfo}
9	Front pendant (final) superheater exit steam enthalpy	h_{fsfo}
10	Main steam header pressure	P_{ms}
11	Reheater exit steam enthalpy	h_{rhfo}
12	Hot reheat header pressure	P_{hr}
13	Gas temperature at economizer exit	T_{ecgo}

3.5.3 Water/Steam Flow Modeling

The simplified water/steam flow path of Figure 3.5-2 shows the key elements to be modeled. Not shown is the feedwater extraction from the HP, IP and LP turbines to the eight feedwater heaters. This flow is small and is modeled as a flow loss from the turbines. The primary assumptions used in modeling the flow are as follows:

1. The flow from the feedwater pump is maintained by a local control loop and can be modeled as a linear function of the flow control setting: $w = 0.01\, U_{bfp} w_{max}$ where w is the water flow (lbm/sec), w_{max} is the maximum flow defined by the control loop, and U_{bfp} is the feedwater pump control that ranges from 0% to 100%.
2. The relationship between flow and pressure drop across pipes and heat exchangers is defined by $w = K_w \sqrt{\rho(P_i - P_o)}$ where ρ is an "average" water density and K_w is a composite flow coefficient. This equation ignores the variation in "pipe friction factor" with Reynolds number (i.e., with velocity), but it was found to be fairly accurate for this application. For modeling heat exchangers where there is a significant change in density from input to output, the "average density" is calculated as the inverse of average input/output specific volume ($v = 1/\rho$), which seems to be somewhat more accurate than the average density or average log mean specific volume. The K factors are computed empirically from plant measurements.

3. Pressure at the economizer inlet and feedwater pump is calculated using the flow equation $P_i = P_o - w^2 / (\rho K_W^2)$ since economizer water outlet enthalpy and drum pressure are model states, and the inlet feedwater temperature is measured.

4. Water leaving the drum in the downcomers enters the circulation pumps, mud drum, and waterwall. Because of the large diameter of the downcomers, the viscous pressure drop in the downcomer is ignored and only the static difference in pressure due to the approximately 100-foot difference in elevation is modeled.

5. The three circulation pumps are modeled using $P_o - P_i = K_A + K_B w + K_C w^2$ where the K constants are obtained from manufacturer data. (Circulation flow is about 3900 lbm/s—about six times larger than feedwater flow.)

6. The flow in the waterwall and risers is modeled using $w = K_w \sqrt{\rho(P_i - P_o)}$ where the static pressure difference is included. The water/steam density changes by a factor of two as it rises (exit quality = 0.15), and average density is much less than that in the downcomers.

7. Flow of saturated steam from the drum through three superheaters to the sprays is modeled by $w = K_w \sqrt{\rho(P_i - P_o)}$. Flow from the spray to the main steam header (inlet to governor valve) is modeled similarly. The main steam header pressure is a state, so pressure at the sprays can be calculated.

8. The time rate-of-change of the main steam header pressure is defined as

$$\dot{P} = \frac{w_i - w_o}{V \left.\dfrac{\partial \rho}{\partial P}\right|_h}$$

where w_i and w_o are input and output steam flow, V is pipe volume, and $\left.\partial \rho / \partial P\right|_h$ is the thermodynamic partial derivatives of density with respect to pressure at constant enthalpy. The volume of the main steam pipes was set greater than the actual volume so that that numerical integration steps greater than 1 s could be used.

9. Flow through the HP turbine is modeled by the governor valve characteristics (manufacturer data) and by "choked flow" through the remaining stages. The choked flow model is $w = K_T \sqrt{P_i \rho_i}$ where P_i and ρ_i are the inlet pressure and density, and K_T is the effective flow coefficient. (Choked flow modeling is discussed in Appendix C.) While the flow may not be fully choked, the turbines behave as if the flow is mainly a function of inlet pressure and density, even with changes in extraction flow.

10. Flow through the IP turbine is equal to the flow through the HP turbine less the extraction flow plus the reheat spray flow, plus leakage from the HP to IP turbine. The reheat spray flow is assumed to be a known function of the spray valve position. Turbine extraction flows are assumed to be a fixed fraction of the total turbine flow and HP-IP leakage flow is also assumed to be a fixed fraction. Since the hot reheat header pressure and enthalpy are model states, the pressure at the reheater inlet can be computed using $w = K_w \sqrt{\rho(P_i - P_o)}$.

11. The flow exiting the IP turbine (input steam less extraction) enters the LP turbine. The pressure at the LP inlet is determined from $w = K_T \sqrt{P_i \rho_i}$ using the flow, density, and flow coefficient.

7

Note that the water/steam circuit was modeled without solving a network of flow equations. Since the inlet flows (feedwater and sprays) were known, and three pressures were states, all flows and intermediate pressures can be computed. This approach should be applicable to most plants if critical flows are measured or can be calculated from valve characteristics.

3.5.4 Air/Gas Flow Modeling

The approach used for water/steam flow modeling depends upon knowing the input flows and using pressures at a few critical locations as states. A slightly different approach is used for the air/gas path. While the input airflow at the El Segundo plant is measured, the gas recirculation flow is not. Had gas recirculation mass flow meters been installed, it would not have been necessary to compute the gas pressures within the furnace. However, since the gas recirculation flow is a function of the pressure across the fans, this model is required.

Because of the need to keep the model order low and to use a 1 s or greater integration time step, the gas pressure states were not included in the state vector. Rather, a small set of flow equations were iterated several times to compute the steady state pressures. This is done at each integration step and it is also done when the model equations are numerically differenced to compute partial derivatives. Because the flow equations are nonlinear, a nonlinear optimization algorithm is used to compute the solution, although only one step is taken when computing partial derivatives.

The assumptions used in modeling the air/gas path flow of Figure 3.5-3 are as follows:

1. Because of balanced operation, both halves of the furnace are treated as one.
2. Because the preheater airflow is measured after passing through the air preheater, and the measurement is used to control the FD fans, flow is modeled as $g = 0.01 U_{fd} g_{max}$, where g is the air mass flow (lbm/s) and U_{fd} is the airflow control.
3. The pressure drop from the FD outlet to the flow sensor is modeled using $g = K_g \sqrt{\rho (P_i - P_o)}$ where ρ is computed using the ideal gas law: $\rho = 144 P / [53.3(T + 460)]$ where ρ is in lbm/ft^3, P is in lbf/in^2 absolute (psia), and T is degrees F. The gas constant 53.3 is based on air with a molecular weight of 28.97. The corresponding constant for gas after combustion is about 55.2 (if fuel is a mixture of methane and ethane). Use of this equation requires that the temperature be known at all nodes of the air/gas path.
4. The flow from the split of the primary and auxiliary ducts to the furnace is modeled as one flow $g = K_g \sqrt{\rho (P_i - P_o)}$, but the flow coefficient is computed by summing the coefficients for the four paths, and including the duct and damper conductance in series. The damper position signals are available on the *distributed control system* (DCS), but the actual damper effective area may not be known precisely, and thus the computation may not be accurate. The flow could be computed more accurately if additional pressure sensors were used in the gas path.
5. The pressure drops from the furnace to the economizer, from the economizer to the stack, and from the gas recirculation fan outlet to the auxiliary air duct is modeled using $g = K_g \sqrt{\rho (P_i - P_o)}$. However the great variation in temperature from furnace-to-economizer requires that the density at each location be computed and averaged. The

temperature at each node is saved after each integration time step and used for the next time step.

6. The gas recirculation fan is modeled by $\alpha = 172.8 \, (U_{grc} - 0.3)^2$, $g = 1/(\rho_g N_{grc} \sin \alpha)$, and $\Delta P = K_A + K_B g + K_C g^2$ where U_{grc} is the gas recirculation control, α is the inlet vane angle in degrees, N_{grc} is the number of gas recirculation fans in use, and ρ_g is the gas density. The first equation is required because a cam is used to counteract the nonlinear effect of the vane angle on flow (approximated by a *sine* function). The resulting flow is approximately a linear function of U_{grc}.

3.5.5 Furnace/Boiler/Drum

Accurate modeling of the furnace and drum is critically important to the success of NMPC because dynamic response times are longer than for other parts of the system. The boiler is modeled using three states: water/steam enthalpy in the risers, drum water enthalpy, drum pressure, and drum water level. Other combinations are also possible. The heat transfer from the flame to the waterwall water is computed using a three zone furnace model: the area above the burners, the burner area, and the area below the burners. The assumptions used in the model are as follows:

1. The total heat available in the fuel is computed as $\dot{Q}_f = g_f h_{lhv}$ where h_{lhv} is the fuel lower heating value and g_f is the flow rate. The adiabatic enthalpy available from the fuel is computed as

$$h_f = \frac{\dot{Q}_f + g_a h_a + g_{grc} h_{grc}}{g_f + g_a + g_{grc}}$$

where g_a and h_a are the inlet airflow and enthalpy respectively, and g_{grc} and h_{grc} are the gas recirculation flow and enthalpy respectively. The weight fraction of water vapor in the combustion products is computed from the constituents of the fuel (which is analyzed periodically). This is then used to compute the adiabatic flame temperature T_f from h_f using thermodynamic property functions.

2. Since computation of the radiant heat transferred to the water/steam involves iterative solution of a set of nonlinear equations, it is necessary to compute an initial guess for the heat transfer. This is computed from the water enthalpy states by assuming that the system is in steady state, $\dot{Q}_g = w_{dc}(h_{ri} - h_{dw})$ where w_{dc} is the water flow in the downcomer, h_{ri} is the enthalpy exiting the risers, and h_{dw} is the enthalpy of the drum water. This is used to compute an initial guess for the exit gas temperature for the burner zone as $T_{go} = T_{gi} - F_1 \dot{Q}_g / (C_p g_{tot})$ where T_{gi} is the adiabatic flame temperature computed above $(= T_f)$, F_1 is the furnace area fraction of the burner section (approximately 0.35 but it also takes into account the number of operational burner elevations), and $g_{tot} = g_f + g_a + g_{grc}$.

3. It is assumed that the radiant heat transferred from the hot gas to the metal can be computed as $\dot{Q}_m = K_r [(T_g + 460)^4 - (T_m + 460)^4]$ where K_r is the radiant heat transfer coefficient, T_g

and T_m are respectively the temperature of the hot gas and metal (°F). Since the second term is much smaller than the first and the water/steam temperature is close to the metal temperature, it is assumed that $T_m = T_{ri}$, where the riser water temperature T_{ri} is computed from h_{ri} and P_{drm}. T_g is an average gas temperature which is computed as a weighted average of the adiabatic flame temperature and the outlet gas temperature for the section $T_g = K_{fc}T_{go} + (1 - K_{fc})T_f$ where K_{fc} has been experimentally determined to be about 0.60. The above equations are combined to obtain the nonlinear relation $g_{tot}C_p(T_{gi} - T_{go}) = F_1 K_r [K_{fc}T_{go} + (1 - K_{fc})T_{gi}) + 460]^4 - (T_m + 460)^4$, which is solved using a single Newton iteration. This is possible because the initial estimate of T_{go} allows the equation to be normalized and converted to a logarithmic form that can be solved directly for a better estimate of T_{go}.

4. A similar procedure is used for the next furnace section (below the burners) where T_{go} from the burner area becomes T_{gi} for this section. The major difference is the calculation of the effective area for the section as $F_2 = 1 - F_1 K_\theta \theta$ where θ is the burner tilt angle and K_θ is the sensitivity of the effective area to burner tilt. K_θ was initially computed from furnace geometry and later estimated from plant pulse testing. The sensitivity is smaller for small flames than for a fully developed fireball. It has also been observed that the effective radiant heat transfer coefficient is smaller at high loads.

5. The time rate of riser water/steam enthalpy change is computed as $\dot{h}_{ri} = [\dot{Q}_T + w_{dc}(h_{dw} - h_{ri})]/K_{mww}$ where w_{dc} is the water flow through the downcomer, h_{dw} is the enthalpy of the drum water, h_{ri} is the riser water/steam enthalpy, and K_{mww} is the effective heat capacity of the waterwall, which is dominated by the metal mass. Several approximations were required to obtain this equation: the energy difference is an average but the enthalpy change is assumed to occur at the outlet.

6. The average density change and outlet flow from the risers is computed as

$$\dot{\bar{\rho}} = -\frac{1}{2}\bar{\rho}^2 \left.\frac{\partial v}{\partial h}\right|_\rho \dot{h}_{ri}$$

where $\partial v/\partial h|_\rho$ is relatively constant and can be easily computed as a function of drum pressure using the approximation $\partial v/\partial h|_\rho = 0.0000392 + (0.62299 - 18.652/P_{DRM})/P_{DRM}$ Then ignoring water/steam slip, $w_{ri} = w_{dc} - V\dot{\bar{\rho}}$.

7. Using a mass balance on the drum water (assuming that separators work perfectly and water is incompressible), the water volume rate-of-change is $\dot{V}_w = [(1-x)w_{ri} + w_{ec} - w_{dc}]/\rho_w$ where w_{ec} is the water flow from the economizer, x is steam quality in the risers, and ρ_w is the density of the drum water. The water level rate-of-change in inches/s is $\dot{l}_w = 12\dot{V}_w/A_w$ where A_w is the effective water surface area at the nominal water level. The area changes slightly with water level but this is ignored.

8. A mass balance on the drum steam gives the change in steam density

$$\dot{\rho}_s = \frac{x\,w_{ri} + \dot{V}_w \rho_s - w_s}{V_{drm} - V_w}$$

where V_{drm} is the total volume of the drum, and w_s is the mass flow rate of the saturated steam to the radiant superheater. Because the riser pipe diameter and the riser volume are large, the riser volume is included as part of the drum volume. The drum pressure change is then computed assuming that the drum steam remains saturated: $\dot{P}_{drm} = \dot{\rho}_s / (\partial\rho / \partial P)$ where $\partial\rho / \partial P$ is the partial of saturated steam density to changes in pressure and can be accurately approximated over the range 100 to 3100 psi as

$$\partial\rho / \partial P = 0.000814 + Y[0.038393 + Y(-0.030599 + 0.019116\,Y)]$$

where $Y = 100 / (3208.2 - P_{drm})$. This equation has been validated for normal plant operations by comparison with alternate models that include an extra state for steam enthalpy.

9. An energy balance on the drum water gives the water enthalpy rate $\dot{h}_{dw} = [w_{ec}(h_{ec} - h_{dw}) + (1-x)w_{ri}(h_f - h_{dw})] / (\rho_w V_w)$ where h_f is the saturated water enthalpy at the given drum pressure.

The above equations are sufficiently accurate for a forced circulation boiler, but whether they are adequate for natural circulation is unknown.

3.5.6 Heat Exchangers

The assumptions used to model heat exchangers are as follows:

1. Heat transfer in the front and side wall radiant superheater, and the platen superheater is assumed to be totally radiant and is modeled using the equations of the previous section (for modeling radiant heat transfer from the hot gas to the steam). The effective radiant transfer coefficient changes slightly with operating point.

2. Heat transfer in the horizontal, rear pendant, and front pendant superheaters, and the reheater is assumed to be entirely convective. While not strictly true, plant data indicate that it is a good assumption. The process is similar to the one used for radiant transfer. First, an initial guess for the outlet gas temperature is computed using the same approach used in the previous section: $T_{go} = T_{gi} - [w(h_{wi} - h_{wo})] / (C_p g_{tot})$ where h_{wi} and h_{wo} are respectively the steam input and output enthalpy, w is the steam flow, T_{gi} and T_{go} are respectively the input and output gas temperatures, and C_p is the constant pressure specific heat of the gas at T_{gi}. g_{tot} used in this equation may be slightly less than the value used for the furnace because of leakage. It is assumed that convective transfer can be modeled as $\dot{Q} = K_c (g / g_{ref})^{0.6} (\overline{T}_g - \overline{T}_f)$ where g_{ref} is the reference gas flow (e.g., maximum flow), K_c is the convective transfer coefficient, $\overline{T}_g$ is an average gas temperature, and $\overline{T}_f$ is an average steam temperature (which should be close to the metal temperature). Most of the convective heat exchangers are counterflow and the appropriate $\overline{T}_g - \overline{T}_f$ is the log-mean temperature difference (see, for example, White 1988):

$$\overline{T}_g - \overline{T}_f = \frac{(T_{gi} - T_{fo}) - (T_{go} - T_{fi})}{\ln[(T_{gi} - T_{fo})/(T_{go} - T_{fi})]}$$

Since these equations are nonlinear, one Newton iteration is used to compute the updated $\dot{Q}$ and T_{go} from the initial estimate. Since the initial estimate is quite accurate, a single iteration is sufficient (even during transients).

3. The exit steam enthalpy rate for each heat exchanger is computed using $\dot{h}_o = [\dot{Q} + w(h_o - h_i)]/K_m$

Since the exit steam enthalpies from the all the heat exchangers are carried as model states, all steam temperatures used in the above equations are available. However, the gas temperatures are not states. Thus, it is necessary to follow the gas path in evaluating the equations. That is, the exit gas temperature from one exchanger becomes the inlet gas temperature for the next. This procedure can even be used for parallel exchangers in the gas path.

3.5.7 Combustion

The fuel used at the El Segundo plant is a mixture of refinery and natural gas, where the hydrogen content of the refinery gas can vary from 0% to 40% by volume. The model can compute the gas composition for arbitrary fuel compositions and air/fuel mixtures. For demonstration purposes, we assume that the fuel is a mixture of ethane and methane. The reaction equation assuming complete combustion is

$$\frac{g_f}{M_f}(f_{CH4}CH_4 + f_{C2H6}C_2H_6) + \frac{g_a}{28.97}\frac{(O_2 + 3.76N_2 + f^a_{H2O}H_2O)}{4.76 + f^a_{H2O}}$$

$$\rightarrow \left[\frac{g_f}{M_f}(f_{CH4} + 2f_{C2H6})\right]CO_2$$

$$+ \left[\frac{g_f}{M_f}(2f_{CH4} + 3f_{C2H6}) + \frac{g_a}{28.97}\frac{f^a_{H2O}}{(4.76 + f^a_{H2O})}\right]H_2O$$

$$+ \left[\frac{g_a}{28.97}\frac{3.76}{(4.76 + f^a_{H2O})}\right]N_2$$

$$+ \left[\frac{g_a}{28.97(4.76 + f^a_{H2O})} - \frac{g_f}{M_f}(2f_{CH4} + \frac{7}{2}f_{C2H6})\right]O_2$$

where g_f is the fuel flow rate (lbm/s), g_a is the airflow rate, f_x is the mole fraction of component x, and $M_f = 16.04f_{CH4} + 30.07f_{C2H6}$. If it is found that that there is insufficient air for complete combustion, the equations are recalculated assuming that the excess air fraction equals zero. This equation was based on the following molecular weights:

CH_4	16.04
C_2H_6	30.07
O_2	31.999
N_2 ("atmospheric")	28.16
CO_2	44.01
H_2O	18.015
Air	28.97

The molecular weight of the combustion products is computed by multiplying the number of moles/s of each constituent by the molecular weight, summing, and dividing by the total number of moles. Since the total weight flow of the combustion products is $g_f + g_a$, the weight fraction of each constituent can be computed by multiplying the number of moles/s of the constituent by the molecular weight and dividing by $g_f + g_a$.

Note that the gas recirculation flow is not included here since it does not affect the equation for that portion of the gas flow due to the input fuel and air (i.e., it has the same composition as the output).

3.5.8 Turbines and Feedwater Heaters

The three turbines have a total of 11 stages, and small amounts of hot steam are extracted from eight points for the purposes of heating boiler feedwater. Use of extracted steam to heat feedwater contributes significantly to overall plant efficiency, but it seriously complicates plant modeling because the extraction flows are not measured. The HP governor stage is also difficult to model.

We previously noted that the effect of turbine exhaust pressure on the flow is very small and the flow can be modeled within about 1% using a "choked flow" model of the form $w = K_T \sqrt{P_i \rho_i}$. This equation is accurate even with changes in feedwater heater extraction, with loss of heater number one having the greatest effect, and downstream heaters having less effect. However this equation only works well for turbine stages after the governor valve.

3.5.8.1 Governor stage

The HP governor (throttling) stage—schematically shown in Figure 3.5-4—consists of four separate parallel valves, where each valve covers an arc of the turbine. As operated at El Segundo, three valves open together and the fourth only opens above 80% flow (Figure 3.5-5). To properly model the flow and efficiency characteristics of the governor stage, it is necessary to model the adiabatic flow through each valve followed by the "isentropic" expansion through the impulse nozzle. Since all valves do not open together, and the relative steam/bucket velocity is different for each nozzle, solution of the flow involves solving a set of four nonlinear equations. This was too computationally intensive for NMPC (although it was used for testing), so an alternate approach was developed.

It was empirically determined that the flow through the HP turbine is proportional to main steam $\sqrt{P_{ms} \rho_{ms}}$ at constant governor valve position. Thus, flow through the turbine was tabulated as a function of governor valve position for nominal operation (2415 psia, 1050 $^\circ$F), and was then scaled by $\sqrt{P_{ms} \rho_{ms}}$ for off-nominal main steam conditions. The flow versus governor valve position was computed using a cubic polynomial fit to the flow/valve position

data. It was also found that the governor stage efficiency versus governor valve position is nearly independent of main steam conditions. This was computed as a tabular function of valve position.
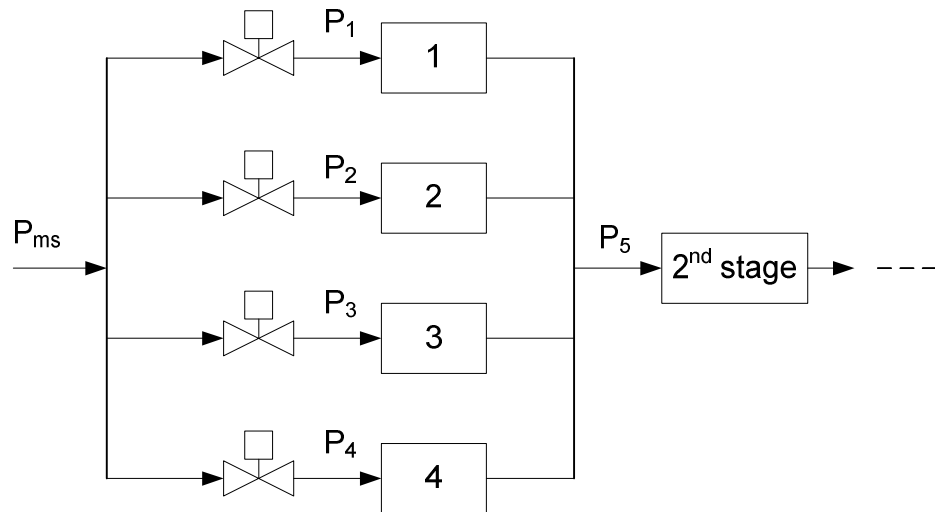
Figure 3.5-4: 4-Arc governor stage of HP turbine.
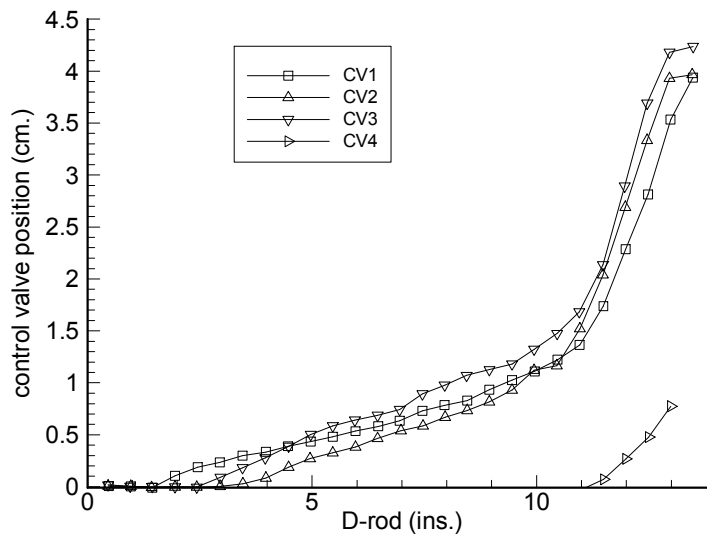
Figure 3.5-5: Governor valve opening.

3.5.8.2 Turbine Stage Flow

Calculation of energy loss through the turbine requires knowledge of pressure at each stage. First stage shell pressure can be computed within 3% as $P_5 = w\sqrt{P_{ms}v_{ms}} \, / \, (1.02\,K_5)$, where v_{ms} is

the main steam specific volume, and K_5 is the flow constant of the first stage after the governor; that is, $w = K_5 \sqrt{P_5 / v_5}$.

Rather than modeling the flow through each individual stage (or between steam extractions), the total flow for each turbine (HP after governor stage, IP, and LP) is modeled. Since the extracted steam is not measured and cannot be easily computed, an approximation is used. The relative steam flow at different extraction points is nearly constant at different loads, with the largest variation occurring in the last two LP extractions. Since the increase in feedwater energy from the condenser to deaerator and boiler feedpump to economizer inlet can be computed (from measured temperatures and flows), the total extraction flow between these points can be computed if the extraction steam enthalpy is known. This can be approximated from main steam and hot reheat conditions. Thus each individual extraction flow can be estimated if the relative flows are known. Although this method is only moderately accurate, the extraction flows are a sufficiently small fraction of total turbine flow that the error is acceptably small. Each extraction flow is subtracted from the turbine exhaust flow in computing the flow to the next turbine, and an average flow is used in computing energy converted to mechanical power. Relative temperatures around the feedwater heaters can be used to determine if heaters are out-of-service, and the extraction ratios can be modified. In addition to feedwater heater extractions, flow leakage of about 1.3% from the HP to IP turbine and leakage from input to output of the HP turbine are also modeled.

If pressure at the inlet and outlet of each turbine is known, the isentropic loss in steam enthalpy can be computed. The isentropic expansion is computed using an ideal gas formulation:

$$\Delta h_{oi} = \left(\frac{0.18505 k}{k-1} \right) P_i v_i \left[1 - \left(\frac{P_o}{P_i} \right)^{(k-1)/k} \right] ,$$

which is accurate within 1% except for the last two LP stages where the maximum error for the stages is 7% and 10% respectively at maximum load. This is true even though these stages operate in the two-phase region. At lower loads the approximation is even better. This is acceptably accurate since the error is only 3% of total generator output at 100% load. The Kalman filter can compensate for errors this small by modifying the turbine efficiency, which is state in the filter model.

3.5.8.3 Turbine efficiency

The turbine output enthalpy is computed as $h_o = h_i - \Delta h_{oi} \eta$ where η is the isentropic efficiency. The power produced by each turbine is calculated (in megawatts) as $P_{MW} = (3.6 / 3412.75) w_{avg} \Delta h_{oi} \eta$, where w_{avg} is an average of the input and output steam flow. η is computed as the maximum turbine efficiency at ideal conditions multiplied by a correction factor for nonideal conditions. That is, maximum efficiency for a single impulse stage is obtained when the bucket velocity is one-half of the steam velocity exiting the nozzle. The efficiency falls off quadratically for other ratios. Salisbury (1974) notes that the efficiency function of large turbines is very close to quadratic, although the location of the peak depends on the stage design. Therefore, we assume that the turbine design conditions at maximum load are

the point of maximum efficiency, and apply a quadratic correction for other conditions. First, the normalized bucket/steam velocity ratio is computed as

$$\frac{V_b}{V_i} = 0.5\sqrt{\frac{\Delta h_{max}}{\Delta h_{oi}}}$$

where Δh_{max} is the isentropic enthalpy drop at full load. Then

$$\eta = 4\frac{V_b}{V_i}\left(1 - \frac{V_b}{V_i}\right)\eta_{max}$$

where η_{max} is the maximum efficiency at full load. (Note that if $\Delta h_{max} = \Delta h_{oi}$, $\eta = \eta_{max}$.)

When computing the output enthalpy of the governor stage, an approximate inlet pressure is computed as if the governor stage is a single nozzle:

$$P_{cv} = w\frac{\sqrt{P_{ms}v_{ms}}}{K_{ms}} = P_5\frac{1.02K_5}{K_{ms}}.$$

Since at full throttle (all valves open) there will be about a 4% pressure loss through the valves, K_{ms} is chosen so that $P_{cv} = 0.96P_{ms}$ at full throttle. P_{cv} is then substituted in

$$\Delta h_{oi} = \left(\frac{0.18505k}{k-1}\right)P_i v_i\left[1 - \left(\frac{P_o}{P_i}\right)^{(k-1)/k}\right]$$

to compute the isentropic change in entropy for the governor stage. Note that P_{cv} only has physical meaning for a single nozzle. If several nozzles operate sequentially in parallel, P_{cv} does not represent the pressure at any nozzle inlet. Thus the isentropic efficiency used in $h_o = h_i - \Delta h_{oi}\eta$ can be greater than 1.0 at partial loads, and decreases with increasing load; that is, it does not represent the true stage efficiency. While this seems counterintuitive, the approach of modeling the stage as a single nozzle appears to be the best compromise between simplicity and accuracy. The error in the approximation seems to be acceptably small.

The above equations for calculating turbine power are most accurate when applied for each turbine stage or section (between extractions). However, it is acceptably accurate to apply the equations to several sections as follows: all HP stages after the governor stage, all IP stages, the first three LP sections, the fourth LP section, and the fifth LP section. The last two LP sections were treated separately because they can operate in the two-phase region. Also, LP moisture and exhaust losses and the effect of high condenser pressure were included using the procedure described by Spencer et al. (1974) and Cotton and Schofield (1970).

3.5.8.4 Generator output

The turbine power calculated above is the gross power. The net power is computed by subtracting boiler feedwater pump power and generator losses. The feed pump power (maximum 5.9 MW) is approximated as a conversion factor times the water flow times the pressure head multiplied by a pump efficiency, η_{bfp}, where $\eta_{bfp} \cong 0.133 + F_{bfp}(0.922 - 0.320 F_{bfp})$ and F_{bfp} is the fractional pump power.

Generator losses are computed as $P_{HPIP-loss} = 0.645 + 0.865 + 1.054(P_{HPIP-MW}/182.77)$, and $P_{LP-loss} = 0.705 + 0.672 + 1.275(P_{LP-MW}/172.89)$, where $P_{HPIP-MW}$ and P_{LP-MW} are the gross generator powers, and coefficients are computed from data in plant heat balance diagrams. Higher hydrogen pressures may increase these losses.

3.5.9 Air Preheater

The Ljungström regenerative drum air preheater used at El Segundo is about 30 feet in diameter, 5 feet in thickness, and rotates at 1 RPM. Hot exhaust gases from the furnace pass through one side of the preheater and convectively heat the metal partitions. As the drum turns, the heated partitions are exposed to the incoming air from the FD fans, and the air is heated.

Analysis showed that a simple model of the air preheater steady-state transfer using the average temperature difference $\Delta T \cong (\overline{T}_{gi} - \overline{T}_{ao} + \overline{T}_{go} - \overline{T}_{ai})/2$ (rather than the log mean) is acceptable. This leads to

$$T_{ao} = \frac{\left[g_a C_{pa} - g_g C_{pg}\left(1 - \dfrac{2}{\alpha} g_a C_{pa}\right)\right]\overline{T}_{ai} + 2g_g C_{pg}\overline{T}_{gi}}{g_a C_{pa} + g_g C_{pg}\left(1 + \dfrac{2}{\alpha} g_a C_{pa}\right)}$$

and

$$T_{go} = (\overline{T}_{ai} - \overline{T}_{gi} + \overline{T}_{ao}) + \frac{2}{\alpha} g_a C_{pa}(\overline{T}_{ao} - \overline{T}_{ai})$$

where T_{ai} and T_{ao} are respectively the input and output air temperatures, T_{gi} and T_{go} are the input and output gas temperatures, C_{pa} and C_{pg} are the constant pressure specific heats for air and gas, $\alpha = K_{ah}(g_a/g_{ref})^{0.8}$, and K_{ah} is a heat transfer coefficient that is computed to be about 270 (and does not vary significantly for different operating points). The preheater has a 30 s lag response to changes in input gas temperature (because of the rotating drum), but this is ignored in the simplified model. The error in the computed temperatures using the above equations is less than 15°F when using values of C_p evaluated at input conditions. Note that this equation computes T_{go} before the air leakage (approximately 10%) is added.

3.5.10   Thermodynamic Properties

The above equations require that water/steam specific volume and temperature be computed as a function of pressure and enthalpy. Standard library functions (RETRAN-02, 1981) are used for this purpose. Also, the constant-pressure specific heat and enthalpy of the combustion products N_2, O_2, H_2O, and CO_2 are also required as a function of temperature. Simple equations are found

in table A.9e of Van Wylen and Sonntag (1986). C_p or h for any gas composition can be computed by summing the weight fractions of C_p or h for each component:

$$C_P = f_{CO2} \frac{\overline{C}_P(CO_2)}{44.01} + f_{H2O} \frac{\overline{C}_P(H_2O)}{18.015} + f_{O2} \frac{\overline{C}_P(O_2)}{31.999} + f_{N2} \frac{\overline{C}_P(N_2)}{28.16}$$

$$h = f_{CO2} \frac{\overline{h}(CO_2)}{44.01} + f_{H2O} \frac{\overline{h}(H_2O)}{18.015} + f_{O2} \frac{\overline{h}(O_2)}{31.999} + f_{N2} \frac{\overline{h}(N_2)}{28.16}$$

3.5.11 Evaluation of State Differential Equations

The preceding sections presented the approaches and equations used to model different subsections of the plant, but it is not yet obvious how these equations define a set of first-order differential equations suitable for use in a Kalman filter or in NMPC. The procedure is as follows:

1) Define the air/gas flow path consisting of boundary conditions, the following nodes and connections between these nodes:
   - FD fan outlet including the effect of outlet fan dampers
   - junction of air heater outlet and gas recirculation
   - furnace cavity
   - economizer outlet
   - gas recirculation fan output
   - air heater outlet to stack
2) Define the relations between flow and pressure between nodes, along with associated coefficients, control actuator positions and known flow leakage. Model options include:
   - fan or pump: $P_i - P_o = k_1 + k_2 g + k_3 g^2$ where P is pressure and g is flow,
   - frictional pressure drop (e.g., duct or pipe): $g = k \sqrt{\rho(P_i - P_o)}$,
   - junction: $g = k_1 \sqrt{\rho_1(P_{1i} - P_{1o})} + k_2 \sqrt{\rho_2(P_{2i} - P_{2o})}$
3) The set of nodes and flow models between nodes defines a flow network that can be linearized and written in matrix form as $\mathbf{A}\mathbf{p} + \mathbf{b} = \Delta\mathbf{f}$ where $\mathbf{p}$ is the vector of node pressures, $\mathbf{b}$ is a vector of fixed flows (if any) at the nodes, $\Delta\mathbf{f}$ is the net input-output flow at each node, and $\mathbf{A} = \partial\mathbf{f}/\partial\mathbf{p}$ is the Jacobian matrix. $\Delta\mathbf{f}$ must be equal to zero when the air/gas flow is in steady-state, and this is a valid assumption because the time constants of the air/gas dynamics are so short compared with thermodynamic time constants. Since $\mathbf{A}$ is a nonlinear function of $\mathbf{p}$, Newton iteration is used to compute the node pressures that make $\Delta\mathbf{f} \cong 0$. The equations are actually solved as an optimization problem to minimize $\|\Delta\mathbf{f}\|$.
4) The water/steam flow from the feedwater pump to the main steam header of the HP turbine is defined in a similar manner. However, it is not necessary to solve a matrix equation in order to compute the flow. Notice that the dynamic model states include drum pressure, drum enthalpy, main steam pressure, and main steam enthalpy. Also note that the feedwater pump and superheater spray flows are known (controlled by a local controller). Hence the water

flow to the drum is directly known. The steam flow exiting the drum can be computed from the average steam density from the drum to the superheater spray and from the spray to the main steam. These average densities are computed as the average of densities at the end points (computed from the heat exchanger enthalpy and pressure states). The resulting quadratic equation is solved for the pressure at the spray, and thus the drum steam flow.

5) Steam flow through the HP turbine is computed using a quadratic model of flow versus governor valve position and then scaled by the main steam $\sqrt{P_{ms}\rho_{ms}}$ divided by a nominal value. Feedwater extraction flows are modeled as a fraction of the turbine flows. The time derivative of main steam pressure (a model state) is calculated as

$$\dot{P}_{ms} = \frac{f_{fpsh} - f_{ms}}{V_{ms}(\partial\rho / \partial P)}$$

where f_{fpsh} is steam flow exiting the front pendant superheater, f_{ms} is the flow through the governor valve, V_{ms} is a fictitious "volume of the main steam header" that is larger than actual so that integration time steps of 1 s can be used.

6) The loss in steam enthalpy through turbine stages is calculated as the isentropic loss multiplied by turbine efficiency, as described in Section 3.5.8. Turbine efficiency η takes into account ideal efficiency (a model state) and nonideal conditions. Power produced by the turbine is calculated as Δh multiplied by average steam flow. Generator losses are included in calculating generator output.

7) Flow and energy through the IP and LP turbine sections is calculated similarly, but flow through the IP turbine is calculated using the choked flow assumption. The pressure rate for the hot reheat header (input to IP turbine) is calculated as for the main steam header.

8) Energy released by the combustion in the furnace is calculated using the fuel lower heating value assuming complete combustion, but the effects of excess or insufficient oxygen are included in the calculation.

9) The enthalpy of the incoming air from the air preheater is calculated using the air/gas flows and inlet temperatures.

10) The energy transfer in the furnace and drum are calculated as defined in Section 3.5.5. Drum steam pressure, enthalpy, water level, and waterwall riser water/steam enthalpy are model states, and time derivatives are calculated as listed in that section.

11) The energy transfer from the hot gas to the steam in each heat exchanger is calculated using the inlet gas temperature, flow rate and C_p, the exit steam enthalpy (a model state) and approximate pressure (obtained by interpolation from known pressure nodes), and the heat transfer (radiant or convective) coefficient for the heat exchanger. The log-mean temperature difference is used to calculate the heat transfer rate. The time derivative of the exit steam enthalpy is calculated as the difference between the radiant/convective heat transfer rate to the steam, and the increase in total steam heat as it passes through the heat exchanger (calculated from exit steam enthalpies and the flow rate). The order of evaluation follows the gas path: radiant superheater, platen superheater, reheater, final superheater, horizontal and rear pendant superheater, and economizer.

The time derivatives ($\dot{\mathbf{x}}$) of the 13 "core" states ($\mathbf{x}$) of Table 3.5-1 are computed as described above. Then $\mathbf{F} = \partial\dot{\mathbf{x}} / \partial\mathbf{x}$ is computed using numerical partial derivatives, but only one iteration of the air/gas flow network is used since the iteration starts with the steady-state solution. Two options are available for integrating $\dot{\mathbf{x}}$ and computing the state transition matrix $\mathbf{\Phi}$ for the

interval between measurements. In the first option, $\dot{\mathbf{x}}$ is integrated using a second-order Runge-Kutta method while $\mathbf{\Phi}$ is computed using a second-order Taylor series. In the second option $\dot{\mathbf{x}}$ and the nonzero elements of $\dot{\mathbf{\Phi}} = \mathbf{F}\mathbf{\Phi}$ are copied into a single vector and integrated using fourth-order Runge-Kutta integration. The maximum allowable integration step is 1 s, so for measurement time intervals greater than 1 s the integration must be repeated as many times as necessary to reach the measurement time. With the step limited to 1 s, the difference between the two integration methods does not have a significant effect on the performance of the Kalman filter or of NMPC. Thus the second-order method is usually employed. When used in the Kalman filter, a small amount of random walk process noise is modeled on each of the core states, and because the computation time interval is small, $\mathbf{Q}_D$ is assumed to be diagonal. Again little gain in performance is obtained when calculating $\mathbf{Q}_D$ using more accurate methods.

3.5.12   Controls

The control variables used in the simplified model are listed in Table 3.5-2. Note that first-order actuator lags were modeled on all controls, with time constants listed. Thus eight lag control states were added to the 13 "core" states in the simplified model for a total of 21 states. A small amount of process noise on the controls was modeled in the Kalman filter to allow for possible actuator backlash and other problems. However, the lag time constants listed in Table 3.5-2 appear to be significantly longer than lags observed from the operating plant, so it may be possible to remove the lag states from the model. This approach to modeling control actuators is mentioned in Chapter 8.

Table 3.5-2: Control Variables

Control	Actuator Time Constant (s)
Airflow	10
Main steam governor valve	5
Feedwater flow	10
Fuel flow	10
Gas recirculation inlet vanes	10
Burner tilt	10
Superheater spray flow	10
Reheater spray flow	10

3.5.13   Measurement Models

The measured quantities available for use in a control system include (but are not limited to) the sensors listed in Table 3.5-3. Also listed are the assumed noise and bias or scale-factor-error (SFE) standard deviations (units are lbm/s, psi, degrees Fahrenheit, and megawatts), and the time constants of any measurement lags. The listed noise standard deviations appear to be slightly pessimistic since plots of the data show very little random variation, except for the flow measurements. Rather, the listed values represent a conservative estimate of the short-term errors.

    The measurement lags and biases/SFEs are included in the Kalman filter as states to be estimated. Thus the total number of Kalman filter states (50) includes 13 core states, 13 plant model flow and turbine efficiency coefficients, 8 control lag states, 5 measurement biases, and 11 measurement lag states. The temperature measurement lag states represent the thermal mass

of the thermowells, while the lag for the O_2 sensor models the periodic update of the analysis. In the former case, the lags may not be long enough to significantly affect the filter, and the analysis updates may not be modeled well as a lag. Thus the lag states could probably be eliminated from the filter. This does not appear to be necessary, however, since the computational time is significantly shorter than that for NMPC optimization.

Table 3.5-3: Measurements

	Measurement	Units	Noise σ	Bias/SFE	Lag τ (s)
1	Airflow	lbm/s	35	2%	-
2	Fuel flow	lbm/s	0.5	2%	-
3	Gas recirculation flow	lbm/s	10	5%	-
4	Feedwater flow	lbm/s	7	2%	-
5	Feedwater pump exit pressure	psig	30	-	-
6	Main steam pressure	psig	24	-	-
7	Hot reheat header pressure	psig	6.0	-	-
8	Drum pressure	psig	25	-	-
9	HP gov. stage shell pressure	psig	20	-	-
10	Drum water level	In	0.5	-	-
11	HP+IP turbine generated power	MW	0.5	-	-
12	LP turbine generated power	MW	0.5	-	-
13	Excess oxygen in exit flue gas	fraction	0.002	-	20
14	Economizer exit water temperature	°F	2	5	3
15	Economizer exit gas temperature	°F	2	5	3
16	Radiant superheater exit steam temperature	°F	2	5	15
17	Rear pendant superheater exit steam temperature	°F	2	5	15
18	Platen superheater exit steam temperature	°F	2	5	15
19	Front pendant superheater exit steam temperature	°F	2	5	15
20	Main steam temperature	°F	2	5	15
21	Cold reheat header steam temperature	°F	2	5	15
22	Reheater inlet steam temperature	°F	2	5	15
23	Hot reheat steam temperature	°F	2	5	15

3.5.14 Model Tuning and Validation

The model described in the previous sections includes about 104 fixed parameters that define the static and dynamic behavior of the model, of which 55 were not accurately known. Two methods were used to determine the parameters. Plant data at a constant load were used in a least-squares fit to determine the coefficients defining model static behavior. Pseudo-random-

binary sequences (PRBS) are sometimes used to identify dynamic model parameters, but this requires special effort by the plant personnel to conduct such a test. Rather, sequential symmetric pulsing of individual controls was used at the El Segundo plant to compute plant dynamic model parameters. In simulation this was found to be just as effective as testing with random inputs. Furthermore, the method is very easy to implement in a plant test, and does not result in plant instabilities. This was used at the El Segundo plant at load levels from 20% to 100%. Sample plots of measured and model-predicted responses to feedwater pump control pulsing are shown in Figures 3.5-6 to 3.5-9. In each plot the "squares" are predicted variables and the "triangles" are measured variables.
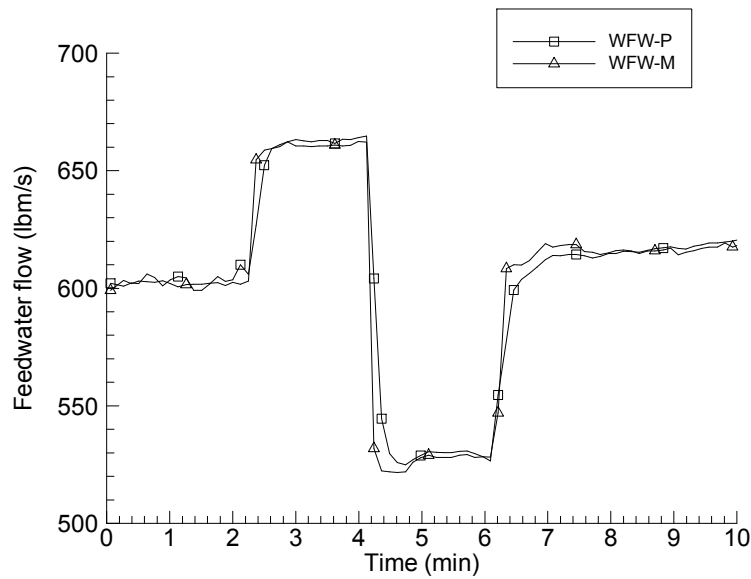
Figure 3.5-6: Feedwater flow response to feedwater pump control pulses at 320 MW.
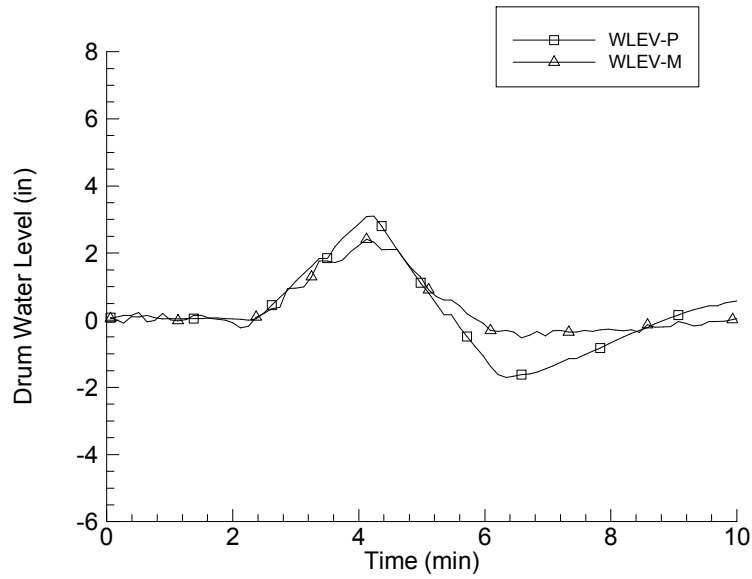
Figure 3.5-7: Drum level response to feedwater pump control pulses at 320 MW.
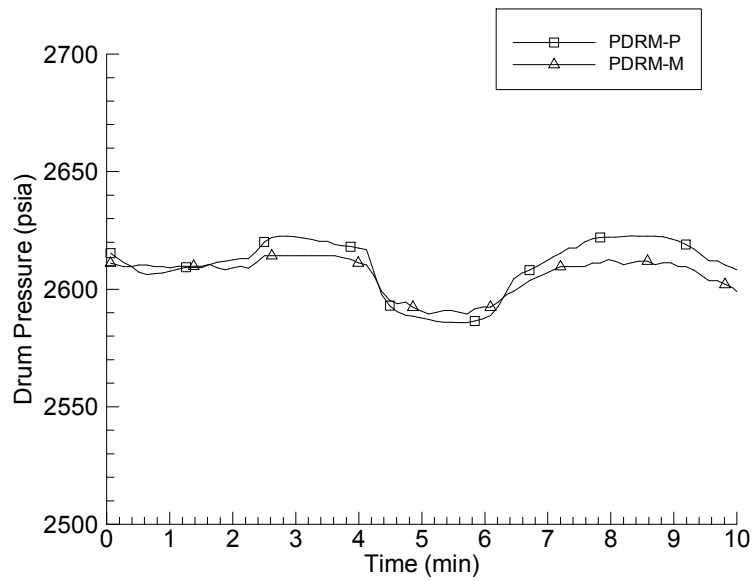
Figure 3.5-8: Drum pressure response to feedwater pump pulses at 320 MW.
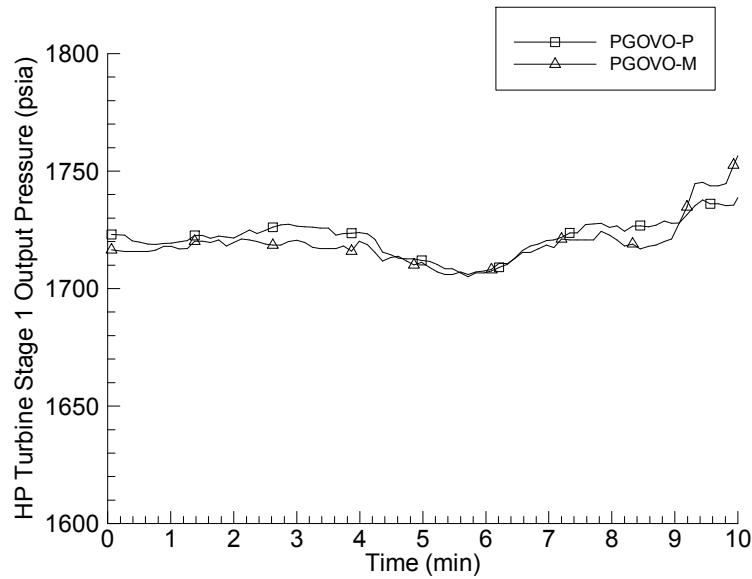
Figure 3.5-9: HP turbine stage 1 output pressure response
to feedwater pump pulses at 320 MW.

Maximum likelihood parameter estimation, discussed in Chapter 11 (also see Schweppe 1973, Åström 1980, Gupta and Mehra 1974, Ljung 1999, 2002, Isermann 1980), was used to compute the fixed dynamic parameters. It is implemented using a Kalman filter to compute the log likelihood function and partial derivatives with respect to the unknown parameters. The method and results for the power plant model are described in Gibbs and Weber (1992a, 1992b). To summarize, the simplified model described in this section was found to accurately model the plant behavior over a wide range in operating conditions, and the NMPC performance for load changes was shown in simulation to be significantly faster than the actual plant using current control algorithms. On the negative side, many man-months of effort were required to develop the model described here. A full understanding of fluid flow, thermodynamics, chemical reaction and control theory was required, in addition to detailed knowledge of the actual plant implementation and performance. This may not be practical for many applications. In some cases additional plant instrumentation would have simplified the model development, but this cannot be expected.